

Development of a Novel Pre-Vascularized Three-Dimensional Skin Substitute Using Blood Plasma Gel

Cell Transplantation
2018, Vol. 27(10) 1535–1547
© The Author(s) 2018
Article reuse guidelines:
sagepub.com/journals-permissions
DOI: 10.1177/0963689718797570
journals.sagepub.com/home/cll


Niann-Tzyy Dai¹ , Wen-Shyan Huang², Fang-Wei Chang³,
Lin-Gwei Wei⁴, Tai-Chun Huang¹, Jhen-Kai Li¹, Keng-Yen Fu¹,
Lien-Guo Dai⁵, Pai-Shan Hsieh¹, Nien-Chi Huang¹,
Yi-Wen Wang⁶, Hsin-I Chang⁷, Roxanne Parungao⁸,
and Yiwei Wang⁸

Abstract

Skin substitutes with existing vascularization are in great demand for the repair of full-thickness skin defects. In the present study, we hypothesized that a pre-vascularized skin substitute can potentially promote wound healing. Novel three-dimensional (3D) skin substitutes were prepared by seeding a mixture of human endothelial progenitor cells (EPCs) and fibroblasts into a human plasma/calcium chloride formed gel scaffold, and seeding keratinocytes onto the surface of the plasma gel. The capacity of the EPCs to differentiate into a vascular-like tubular structure was evaluated using immunohistochemistry analysis and WST-8 assay. Experimental studies in mouse full-thickness skin wound models showed that the pre-vascularized gel scaffold significantly accelerated wound healing 7 days after surgery, and resembled normal skin structures after 14 days post-surgery. Histological analysis revealed that pre-vascularized gel scaffolds were well integrated in the host skin, resulting in the vascularization of both the epidermis and dermis in the wound area. Moreover, mechanical strength analysis demonstrated that the healed wound following the implantation of the pre-vascularized gel scaffolds exhibited good tensile strength. Taken together, this novel pre-vascularized human plasma gel scaffold has great potential in skin tissue engineering.

Keywords

endothelial progenitor cell (EPC), vascularization, 3D skin substitute, plasma gel scaffold, keratinocyte

¹ Division of Plastic and Reconstructive Surgery, Department of Surgery, Tri-Service General Hospital, National Defense Medical Center, Taipei, Taiwan, R.O.C.

² Plastic and Reconstructive Surgery, Zouying Branch of Kaohsiung Armed Forces General Hospital, Kaohsiung, Taiwan, R.O.C.

³ Department of Obstetrics & Gynecology, Tri-Service General Hospital, National Defense Medical Center, Taipei, Taiwan, R.O.C.

⁴ Division of Plastic and Reconstructive Surgery, Taoyuan Armed Forces General Hospital, Taoyuan, Taiwan, R.O.C.

⁵ Department of Orthopedics, Shuang Ho Hospital, Taipei Medical University, New Taipei, Taiwan, R.O.C.

⁶ Department of Biology and Anatomy, National Defense Medical Center, Taipei, Taiwan, R.O.C.

⁷ Department of Biochemical Science and Technology, National Chiayi University, Chiayi, Taiwan, R.O.C.

⁸ Burns Research Group, ANZAC Research Institute, Concord Hospital, University of Sydney, New South Wales, Australia

Submitted: June 2, 2018. Revised: August 8, 2018. Accepted: August 8, 2018.

Corresponding Authors:

Niann-Tzyy Dai, Division of Plastic & Reconstructive Surgery, Department of Surgery, Tri-Service General Hospital, National Defense Medical Center, No. 325, Section 2, Cheng-Kung Road, Nei-Hu District, Taipei 114, Taiwan, R.O.C.; Yiwei Wang, Burns Research Group, ANZAC Research Institute, Concord Hospital, University of Sydney, Concord West, NSW 2137, Australia.

Emails: niantzyydai@gmail.com; yiweiwang@anzac.edu.au



Creative Commons Non Commercial CC BY-NC: This article is distributed under the terms of the Creative Commons Attribution-NonCommercial 4.0 License (<http://www.creativecommons.org/licenses/by-nc/4.0/>) which permits non-commercial use, reproduction and distribution of the work without further permission provided the original work is attributed as specified on the SAGE and Open Access pages (<https://us.sagepub.com/en-us/nam/open-access-at-sage>).

Introduction

The repair of large extensive venous ulcers, burns and diabetic wounds requires hospitalization that results in a reduced quality of life and substantial socio-economic burden^{1,2}. Autografts are the gold standard treatment for wound repair, but are impractical for extensive wound treatments due to the limited availability of donor sites and the risk of secondary morbidity resulting from graft harvesting³. Biomaterial or biopolymer-based skin substitutes have been well developed and investigated in the past decades, including naturally derived polymers (alginate, gelatin, collagen, chitosan, fibrin and hyaluronic acid), synthetic molecules (polyethylene glycol, PEG) or their cross-linking agents^{4,5}. Biomaterial-based scaffolds have been proven to promote cell infiltration and cytokine production, which provides physiological conditions that are favorable for tissue repair post injury^{6,7}. Skin substitutes are usually prepared by seeding with fibroblasts and/or keratinocytes into the respective layers of the scaffold⁸. However, the lack of vascularization inside the scaffolds causes cell death due to hypoxia, which results in a hollow skin substitute. This issue remains a major challenge and limits the potential of these scaffolds for clinical applications.

Previous studies have demonstrated that pre-vascularized scaffolds perform better *in vivo* and facilitate to integrate with the host vasculature⁹. Angiogenesis is a complex biological process involving the activation of endothelial progenitor cells (EPCs) for the regeneration of new blood vessels. EPCs have recently attracted great attention for inducing neovascularization in tissue engineering applications, particularly for clinical applications of autologous cell transplantation¹⁰. In addition, the three-dimensional (3D) environment is important for the formation of the vascularization network as it provides oxygen supply and nutrient exchange to maintain the engrafted tissue. Biomaterial and biopolymer-based scaffolds face the challenge of providing an appropriate microenvironment to maintain cell proliferation, function and cell differentiation of EPCs¹¹.

In the present study, we produced and examined a novel artificial 3D skin substitute using human plasma that was aimed to induce skin regeneration. This umbilical cord blood (UCB) plasma gel provides a favorable 3D microenvironment for fibroblasts and EPCs to contribute to epidermal migration, collagen deposition and wound repair. In addition, 3D plasma gels are sourced from patients individually, so the risk of pathogen transmission or foreign body rejection is eliminated.

Materials and Methods

Culture of Endothelial Progenitor Cells

The isolation and culture of EPCs were performed as previously described with modifications¹². In brief, human UCB was layered on the top of Ficoll-PaqueTM PLUS (GE Healthcare, Chandler, Arizona, USA) followed by centrifugation at

900 g for 30 min. The white layer including mononuclear EPCs was transferred to a new centrifuge tube and subsequently incubated with RBC lysis buffer (Gibco, Paisley, Scotland, UK) for 5 min followed by centrifugation. The lower layer of cells was harvested and suspended in 10 ml of HBSS (Gibco). Cells were washed and incubated with 6 ml of EBM-2 culture medium supplemented with EGM-2 (Lonza, Basel, Switzerland) and 1% antibiotic-mycotic (Sigma-Aldrich, St. Louis, Missouri, USA). The cell solution was pipetted into the fibronectin (Millipore, Billerica, Massachusetts, USA)-coated plate for 2 days to obtain primary EPCs. Primary EPCs between the second and fifth passage were used in the experiment. The expression of specific endothelial progenitor markers including CD31, C-Kit, Tie-2 and VE-Cadherin (Abcam, Cambridge, Massachusetts, USA) was examined to confirm the phenotype of EPCs prior to the study. The study protocol was reviewed and approved by the Institutional Review Board (IRB) in the Tri-Service General Hospital, R.O.C. (TSGHIRB No. 100-05-251). A written informed consent according to the IRB guidelines was obtained from each donor.

The Preparation and Biocompatibility of Plasma Gel

The schematic experimental procedures of cell-contained plasma gel scaffold are presented in Fig. 1. Human blood samples were centrifuged at 800 g for 30 min to separate the plasma from blood cells. The plasma was then filtered through a 0.22 μ m filter (Millipore) to remove impurities. To generate the bottom layer of the plasma gel scaffold, 0.5 ml of plasma was mixed with 0.5 ml of culture medium in a 6 cm culture plate, and then treated with various concentrations (2.5, 5, 10, 20 and 40 mM) of CaCl_2 (5 μ l, Sigma-Aldrich) at 37°C to determine the optimal agglutination condition for the plasma gel scaffold. To form the top layer of the plasma gel scaffold, the plasma was mixed with culture medium containing 1×10^5 cells of human dermal fibroblasts from foreskin (passage 3–5) and then treated with different concentrations of CaCl_2 . Cell growth in the plasma gel scaffold was measured at 6, 12, 24, and 48 h after cell seeding.

Preparation of Pre-Vascularized 3D-Gel Scaffold and Cell Proliferation Assay

EPCs and fibroblasts at various ratios were mixed with 250 μ l of plasma gel in a 24-well culture plate and incubated in co-culture medium to form pre-vascularized 3D-skin substitutes. Typically, 2% FBS containing EBM-2 medium is used to induce the differentiation of EPCs to endothelial cells. In this experiment, EPCs and fibroblasts were mixed prior to seeding into the 3D-plasma gel scaffolds and co-cultured for 7 days to construct a pre-vascularized skin substitute. The co-culture medium was made up of equal amounts of DMEM-High glucose/F12 medium (3:1) and EBM-2 medium containing 1% PSA and 2% (or 20%) FBS. After

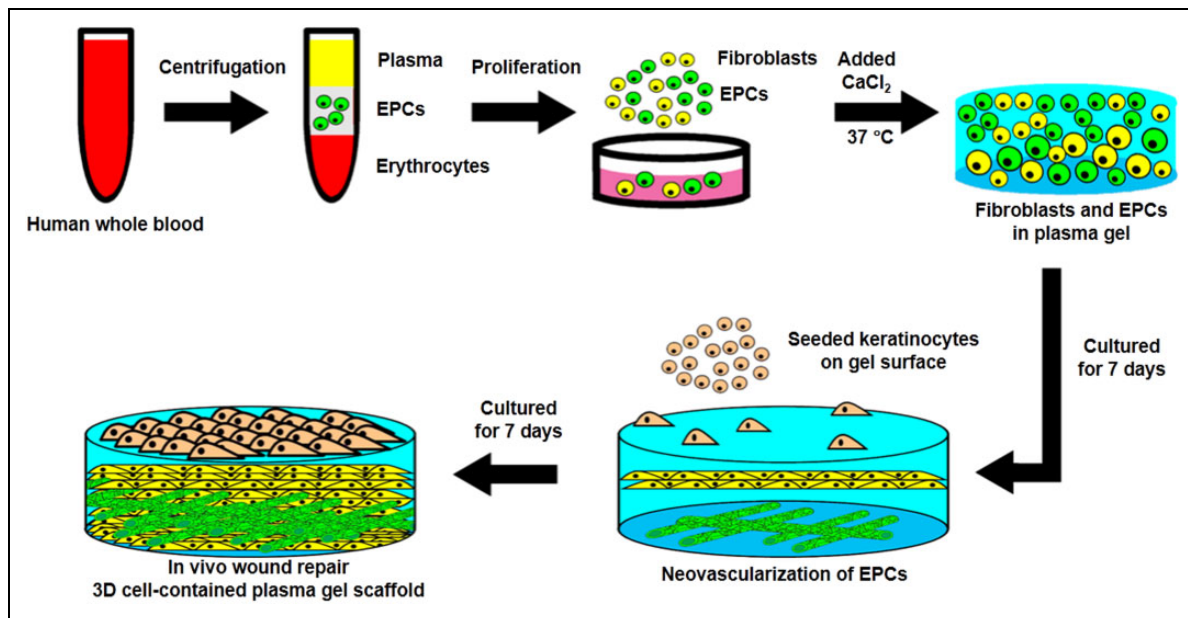


Fig. 1. The schematic diagram for the preparation of cell-contained 3D plasma gel scaffold. After centrifugation, the endothelial progenitor cells were isolated from whole blood and mixed with fixed concentrations of CaCl_2 for solidification. Endothelial progenitor cells proliferated and differentiated for 7 days to form microvascular-like structures, and keratinocytes were then seeded onto the surface of the plasma gel for 7 days to produce the epidermal layer. The cell-containing 3D plasma gel was prepared and then tested using a wound repair model on the dorsal skin of mice.

7 days, keratinocytes were seeded at the density of 1×10^6 cells/cm² onto the external surface of plasma gel scaffolds and incubated for another 7 days. The co-culture medium was prepared with equal amounts of DMEM/F-12 medium (3:1, containing 5% FBS, 1% penicillin/streptomycin, 5 mg/ml insulin, 0.4 mg/ml hydrocortisone, and 1 mM isoproterenol) and EBM-2 medium (supplemented with 1% PSA and 20% FBS). In this study, the pre-vascularized skin substitute contained populations of EPCs, fibroblasts and keratinocytes that were seeded on the plasma gel. Non-vascularized skin substitutes, however, only contained fibroblasts and keratinocytes that were seeded on the plasma gel.

Cell proliferation of EPCs and fibroblasts in the plasma gel scaffolds were determined by WST-8 assay (Dojindo Laboratories, Kumamoto, Japan) at days 1, 3, 5 and 7. In brief, the medium was replaced with 300 μl of WST-8 reagent solution (90 μl WST-8 solution and 210 μl co-culture medium). After incubating with WST-8 reagent solution for 2 h, the absorbance was measured on a microplate reader (Sjeia Auto Reader II; Sanko Junyaku, Tokyo, Japan) with a test wavelength at 450 nm and a reference wavelength at 630 nm. Cell number was then derived using a standard curve. The differentiation of EPCs to endothelial cells was confirmed using an immunohistochemistry assay. As the ratio of EPCs to fibroblasts is a critical factor associated with the vascularization of EPCs, the cells were co-cultured at EPC:fibroblast ratios of 1:0.5, 1:1 and 1:2 in the plasma gel scaffolds. The morphology of EPC-derived endothelial cells was observed by an immunohistochemistry assay using CD31 antibody (ab9498, Abcam).

Immunohistochemistry Assay

Primary EPCs isolated from human UCB were incubated for 3 weeks before confirming the EPC phenotype using a CD31 marker for immunofluorescent staining. Cells were washed with phosphate buffered saline (PBS) twice and fixed in 4% paraformaldehyde (Sigma-Aldrich) for 24 h. The plasma gel was immersed in 100% alcohol for 1 min, washed with PBS three times, and then blocked with blocking buffer ($1 \times$ PBS containing 5% BSA and 0.3% Triton X-100) at room temperature for 1 h. The plasma gel was then incubated with primary mouse monoclonal anti-human CD31 antibody (1:200 dilution) overnight at 4°C, and subsequently with a secondary alexa-conjugated 488 donkey anti-mouse IgG (ab150105, 1:100 dilution, Abcam) overnight at 4°C. The cell nuclei were stained with DAPI (Thermo Fisher Scientific, Waltham, Massachusetts, USA).

In Vivo Animal Studies

In vivo studies using a skin wound healing model in nude mice were performed as previously described¹³. The protocol was approved by the Institutional Animal Care and Use Committee (IACUC) in National Defense Medical Center, Taiwan, R.O.C. (IACUC-14-286). Eight-week-old nude mice (BALB/c-nu; BioLASCO, Taipei, Taiwan) were anesthetized and a full-thickness cutaneous wound (diameter 1.5 cm) was surgically created on the dorsum of the mice. All the surgical instruments were sterilized and the surgical procedures were performed under laminar flow. The surgical

sites were sterilized with Easy Antiseptic Liquid 2% (Panion & BF, Taipei, Taiwan) before surgery. The mice were assigned to one of four treatment groups including blank, plasma gel, non-vascularized skin and pre-vascularized skin. The plasma gel scaffolds were placed on the wounds, sewn into place with 10–12 stitches using NC125 L Nylon 5-0 surgical sutures (UNIK, Taipei, Taiwan), and covered with Tegaderm film (3 M Health Care, St. Paul, Minnesota, USA). The wounds were continuously monitored over a period of 14 days. After 7 and 14 days, the wound tissues were excised, fixed with 10% formalin for at least 24 h at room temperature, embedded in paraffin, and then sectioned in 5- μ m increments. The sections were stained with H&E staining and observed under an optical microscope (ZEISS Axio Scan.Z1, Carl Zeiss, Jena, Germany). Masson's trichrome staining was performed under standard experimental procedures to compare the gross morphology of collagen fibers between the experimental and blank groups. The thickness of the epidermis and dermis was examined using ZEN software. In addition, immunohistochemical analysis was performed on skin sections on day 14 post-surgery with an anti-smooth muscle actin antibody and anti-PECAM/CD31 antibody, to confirm the expression of smooth muscle cells and endothelial cells, which are components of blood vessels. The double stain kit (TADS03, BIOTnA Biotech, Taoyuan, Taiwan) that could detect smooth muscle cells (containing HRP Green Chromogen) and endothelial cells (containing DAB Brown Chromogen) on the same section slide was used following the manufacturer's protocol.

Tensile Tests

Mechanical properties were determined by using a universal testing machine (HT-8504 Hung Ta Instruments, Taichung, Taiwan) on the tensile mode setting. After 14 days post-surgery, the mice were sacrificed and the skin of the dorsal wound was excised. Each skin tissue was cut into a rectangular section of 1.5 cm \times 4 cm. Tissue specimens were stretched at a crosshead speed of 50 mm/min until rupture. Young's modulus and tensile strengths at breakage were calculated from the stress-strain data¹⁴. Six specimens per experimental group were measured to obtain the average values.

Angiogenesis Assay

To assess angiogenesis in the untreated control, plasma gel, non-vascularized and pre-vascularized groups 14 days after implantation, animals were intravenously injected with AngioSense 750 EX (Perkin Elmer, Waltham, Massachusetts, USA; 2 nmol/100 μ l prepared in sterile PBS) via tail vein injection¹⁵. Fluorescence imaging (excitation: 745 nm; emission: 800 nm; high-pass filter cut off: 770 nm; illumination: 30%) in the anesthetized animal was performed 24 h after the injection of the fluorescence dye, using the IVIS Spectrum Imaging System (Perkin Elmer)¹⁵.

Statistical Analysis

Results were presented as the mean \pm standard deviation of three replicates for each experiment. Statistical analysis was performed using SPSS version 22 for Windows (SPSS Inc., Chicago, Illinois, USA). The statistically significant differences between groups were assessed by one-way analysis of variance (ANOVA) with Tukey's HSD Post Hoc Test. $P < 0.05$ was considered statistically significant.

Results

Preparation of the Plasma Gel Scaffolds

The gel scaffolds were prepared by using a series of CaCl_2 concentrations at 2.5, 5, 10, 20 and 40 mM, into a mixture of equal amounts of plasma and culture medium (Fig. 2). Our results demonstrated that 10, 20, and 40 mM CaCl_2 were able to induce agglutination of the plasma gel, but 2.5 and 5 mM CaCl_2 were too low to successfully form the gel (Fig. 2A). Cell proliferation of fibroblasts inside the plasma gel scaffolds was analyzed using WST-8 assay (Fig. 2B). We found that 40 mM CaCl_2 significantly inhibited cell growth from 12 h to 48 h, resulting in cell numbers decreasing from 1×10^5 cells at 0 h to 0.94×10^5 cells at 48 h. In contrast, an increase in cell number from 1×10^5 cells (0 h) to 2.07×10^5 cells (48 h) was observed in plasma gel scaffolds prepared using 10 mM CaCl_2 (Fig. 2B). Therefore, plasma gel scaffolds prepared with 10 mM CaCl_2 were used in the following experiments. This plasma gel scaffold is translucent and gelatinous, and can be easily handled and detached from a 6 cm dish plate after casting.

Pre-Vascularization Using EPC Incorporated Plasma Gel Scaffolds

Primary EPCs were isolated and harvested from UCB samples. First, EPC phenotypes were identified using specific markers of endothelial progenitors such as CD31 (Platelet endothelial cell adhesion molecule), C-Kit (stem cell marker that is found in EPCs), Tie-2 (endothelial cell-specific tyrosine kinases 2) and VE-Cadherin (an endothelial-specific cell–cell adhesion molecule) in the present study (see Supplement S1). After 3 weeks of culture, the expression of CD31 surface bio-markers on EPCs was confirmed using immunofluorescence staining (Fig. 3). To determine if EPCs have the potential to differentiate into vascular-like endothelial cells in a 3D environment, EPCs were cultured in DMEM-High glucose: F12 (3:1 v/v) 2% or 20% FBS medium. As shown in Fig. 3A, a greater extent of vascularization was observed when EPCs were cultured in 20% FBS medium compared with 2% FBS culture medium over 7 days. Furthermore, cell proliferation assay results demonstrated that the cell growth of EPCs was significantly inhibited in the medium containing 2% FBS compared with 20% FBS medium (Fig. 3B). In contrast, the cell growth of fibroblasts was not affected by the concentration of FBS,

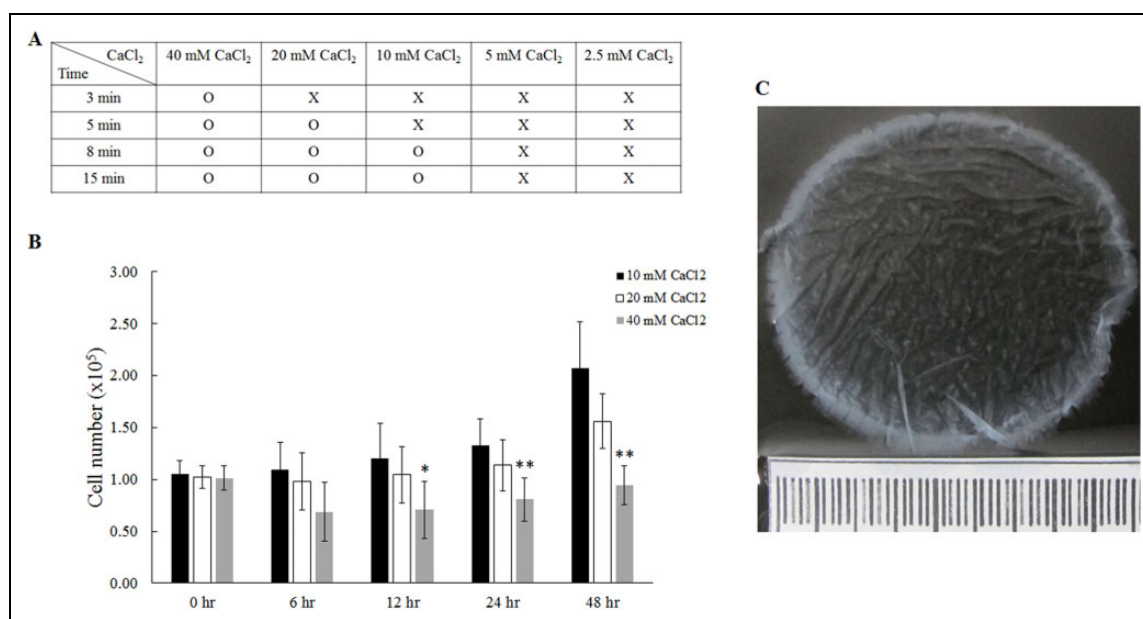


Fig. 2. The preparation of plasma gel with addition of different concentrations of CaCl₂. (A) The effect of plasma agglutination was tested by different concentrations of CaCl₂. (B) The proliferation of fibroblasts for up to 48 h was investigated using plasma gel containing varying specific concentrations of CaCl₂. (C) The morphology of plasma gel containing 10 mM CaCl₂. *: indicates $P < 0.05$; **: indicates $P < 0.01$ when compared with plasma gel with 10 mM CaCl₂.

resulting in very similar rates of cell growth from day 1 to day 7 (Fig 3C).

Pre-Vascularization of EPC on the Plasma Gel Modulated by Fibroblast

The differentiation of EPCs for vascularization was examined in co-culturing conditions with fibroblasts at varying ratios of 1:0.5, 1:1 and 1:2. Positive staining of CD31 was used to assess vascularization of EPCs in the plasma gel (Fig. 4A). The density of vascularized area significantly increased when EPCs and fibroblasts were cultured at a ratio of 1:0.5 over 7 days. On day 3, the vascularization area was calculated at 17.83% and increased to 25.31% by day 7. In contrast, when EPCs: fibroblasts were cultured at either 1:1 or 1:2, the vascularized area was relatively low at approximately 9–12% over 7 days (Fig. 4B).

The Wound Repair by Neovascularized 3D Skin in Nude Mice

To assess the effect of this pre-vascularized 3D skin substitute on wound healing *in vivo*, we used a nude mouse wound healing model. On day 0, all gel scaffolds were able to tightly stitch onto the wound edges. The wound areas of mice grafted with the blank or the plasma gel slowly healed over 14 days (Fig. 5A-a, 5A-e, 5A-i). The wound area contained a wet surface, indicating that the epidermis and dermis has been only partially formed. In contrast, wound healing was accelerated in mice grafted with non-vascularized 3D

skin substitutes (Fig. 5A-c, 5A-g, 5A-k) or pre-vascularized 3D skin substitutes (Fig. 5A-d, 5A-h, 5A-l) on day 7 and 14 post-surgery. Histological analysis showed that both non-vascularized and pre-vascularized 3D gels were well integrated with surrounding tissue compared with the blank and plasma group 7 days post-surgery (Fig. 6A-day 7). Pre-vascularized 3D gels were found to induce an abundant neo-vascularized network in the central wound area (Fig. 6/day7-B-d). Histological analysis further confirmed that all gel scaffolds were well tolerated in the mice, with mild inflammatory responses, and no cell necrosis and apoptosis observed on day 7 and 14 (Fig. 6-day 7 and day 14). The non-vascularized/pre-vascularized 3D skin graft was replaced with the cutaneous construction at the study site, and the neo-vascularized network also achieved a condition of homeostasis. In addition, an epithelial layer formed at the wound site of mice grafted with non-vascularized/pre-vascularized 3D skin substitutes.

Masson's trichrome staining (Fig. 7A) was conducted to assess collagen formation post skin excision and grafting. Wounds grafted with pre-vascularized 3D skin substitutes displayed well-organized collagen fibers with corrugated structure. However, in the blank (Fig. 7A-b) and plasma gel scaffold treatment (Fig. 7A-c) groups, the density of collagen fibers found at the wound site was low. By day 14, more collagen fibers were obviously apparent in the non-vascularized (Fig. 7A-i) and pre-vascularized (Fig. 8A-j) gel groups compared with the other groups. The quantitative analysis of collagen density demonstrated that collagen production in non-vascularized and pre-vascularized groups

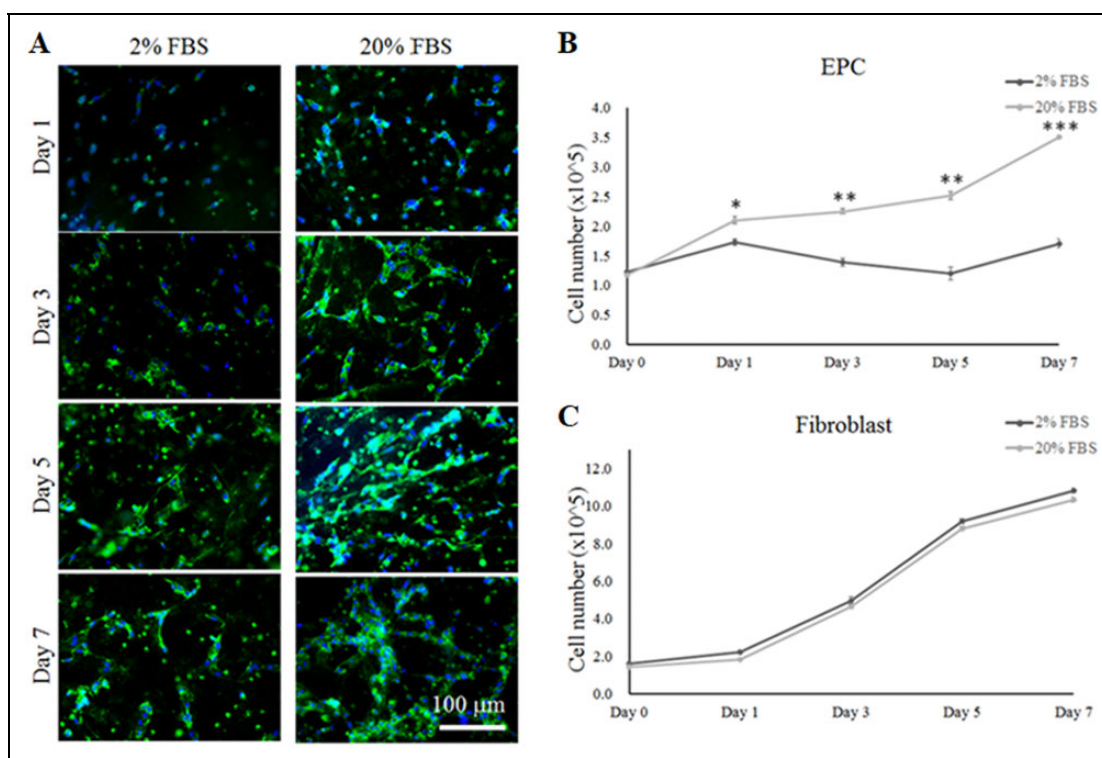


Fig. 3. The differentiation and proliferation of EPCs and fibroblasts in plasma gel in co-culture medium containing 2% or 20% FBS. (A) Immunofluorescent staining for the pre-vascularization of EPCs using a labeled CD31 marker in plasma gel with the different co-culture media at 1, 3, 5 and 7 days. (B) The proliferation of EPCs in co-culture medium was observed at 1, 3, 5 and 7 days. (C) The proliferation of fibroblasts in co-culture medium was investigated at 1, 3, 5 and 7 days. *: indicates $P < 0.05$; **: indicates $P < 0.01$; ***: indicates $P < 0.001$ when compared with the co-culture medium containing 2% FBS.

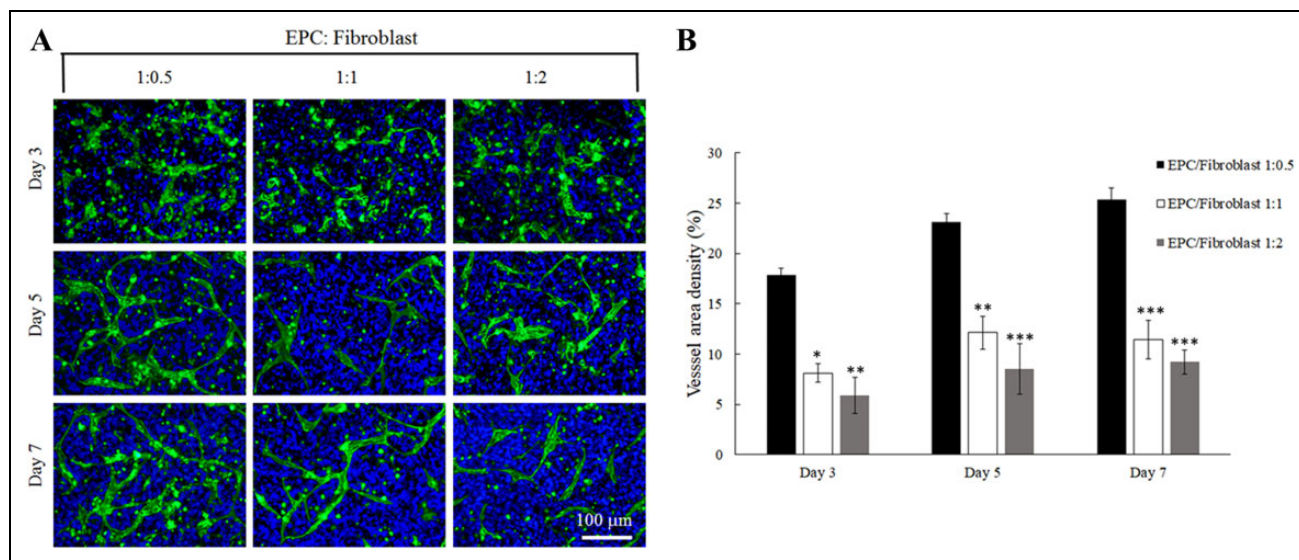


Fig. 4. The differentiation of EPCs under different ratios of EPCs to fibroblasts in plasma gel. (A) Immunofluorescent staining presenting a vascular-like tubular structure from EPCs were labeled with CD31 marker and cell nuclei were labeled with DAPI at 3, 5, and 7 days. (B) The calculation of the vessel density by Image J Software. *: indicates $P < 0.05$; **: indicates $P < 0.01$ when compared with 0.5:1 ratio of fibroblasts to EPCs group.

was significantly higher compared with the blank and plasma gel groups 14 days post-surgery (Fig. 7B). The thickness of the epidermis layer in the central area of the wounds

was measured using a ZEN slidescan tool 14 days post-surgery (Fig. 7C). The thickness of the regenerated epidermis was significantly greater in the non-vascularized

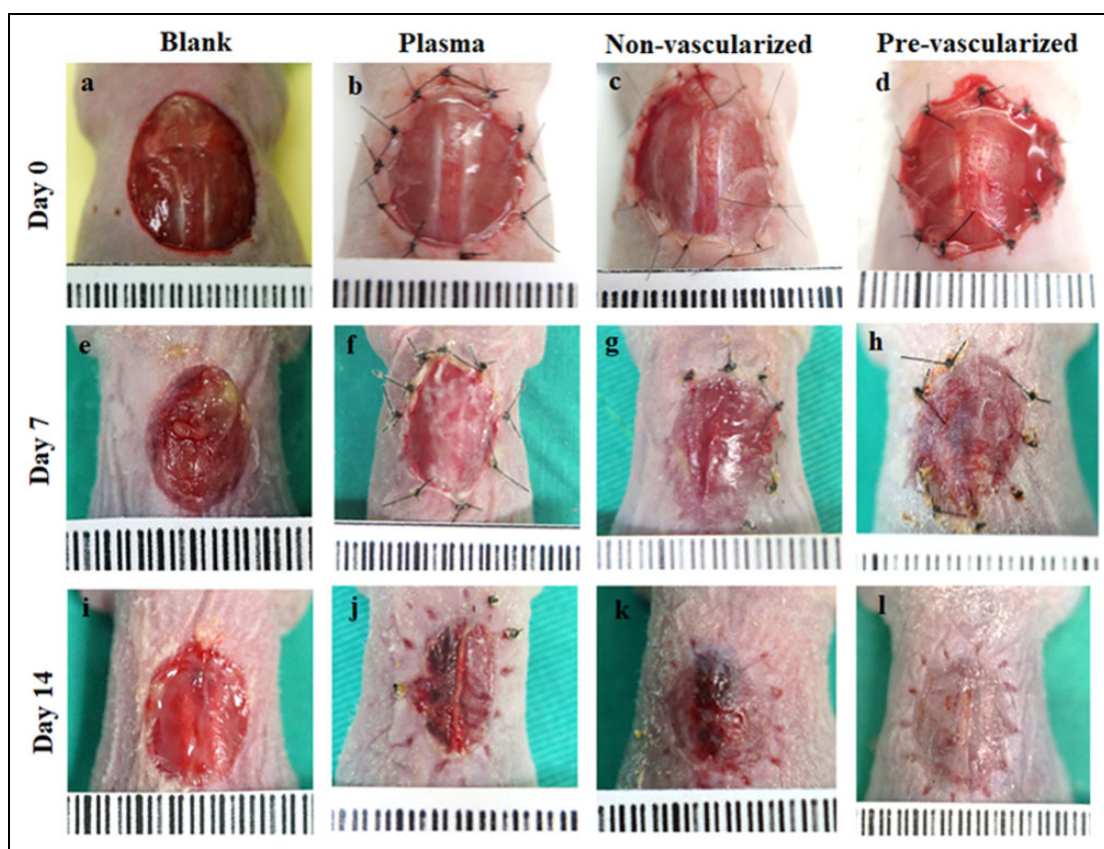


Fig. 5. The *in vivo* wound repair model and angiogenesis located at the dorsal area of nude mice. The observation of wound repair was performed at 0, 7 and 14 days post-surgery. The blank (a, e, i) was not engrafted with any artificial skin. The plasma gel (b, f, j), non-vascularized (c, g, k) and pre-vascularized (d, h, l) were engrafted into the wound.

3D gel-treated wounds, but the thickness of the epidermis was found to be similar between the wounds grafted with pre-vascularized skin substitute and normal skin. Blank or plasma gel scaffold-treated wounds displayed limited re-epithelialization in 14 days. The thickness of the dermis layer was also examined 14 days post-surgery (Fig. 7D). Dermal thickness was significantly increased in the non-vascularized 3D gel-treated group, but not in the pre-vascularized groups. Thinner dermal thickness was observed in the blank and plasma gel groups.

Evaluation Skin Wound Restoration by Tensile Test

The mechanical strength of healed skin was determined using a universal testing machine (Fig. 7E and F). In the blank group, the wound area was not healed on day 14, therefore the strength assessment could not be performed for the blank group. The epidermal layer also could not be found in the blank group, as shown in the histological analysis (Fig. 6A–a). Non-vascularized and pre-vascularized healed skin maintained a similar Young's modulus and tensile strength as normal skin. However, a significant reduction in Young's modulus of 0.66 MPa and tensile strength of 0.22 MPa was observed in the skin healed following plasma scaffold treatment.

Angiogenesis

In order to assess the angiogenesis in the wound area, fluorescence probes (AngioSense 750 EX) were injected on day 14 and fluorescence imaging was recorded 24 h after the injection (Fig. 8A). The highest accumulation of Angiosense 750 fluorophores was found on the wound areas in the pre-vascularized skin group, indicating the formation of functional neovasculature for the regulation of blood flow (Fig. 8A). In addition, non-vascularized skin substitutes showed secondary high fluorescence signals compared with the blank or plasma groups, suggesting that the co-culture of fibroblast may benefit microvascular formation. Furthermore, wounds grafted with non-vascularized and pre-vascularized substitutes formed an epidermis on the surface of wound area. The differentiation of EPCs into smooth muscle cells was further examined using immunohistological double-staining analysis (Fig. 8B). In a normal control skin section, CD31 signals are shown in brown and α SMA expression was shown in green. However, only CD31 (shown as brown) expression was observed in pre-vascularized skin substitutes on day 14, indicating that EPC did not differentiate into smooth muscle cells in the 3D plasma scaffolds during the wound healing process.

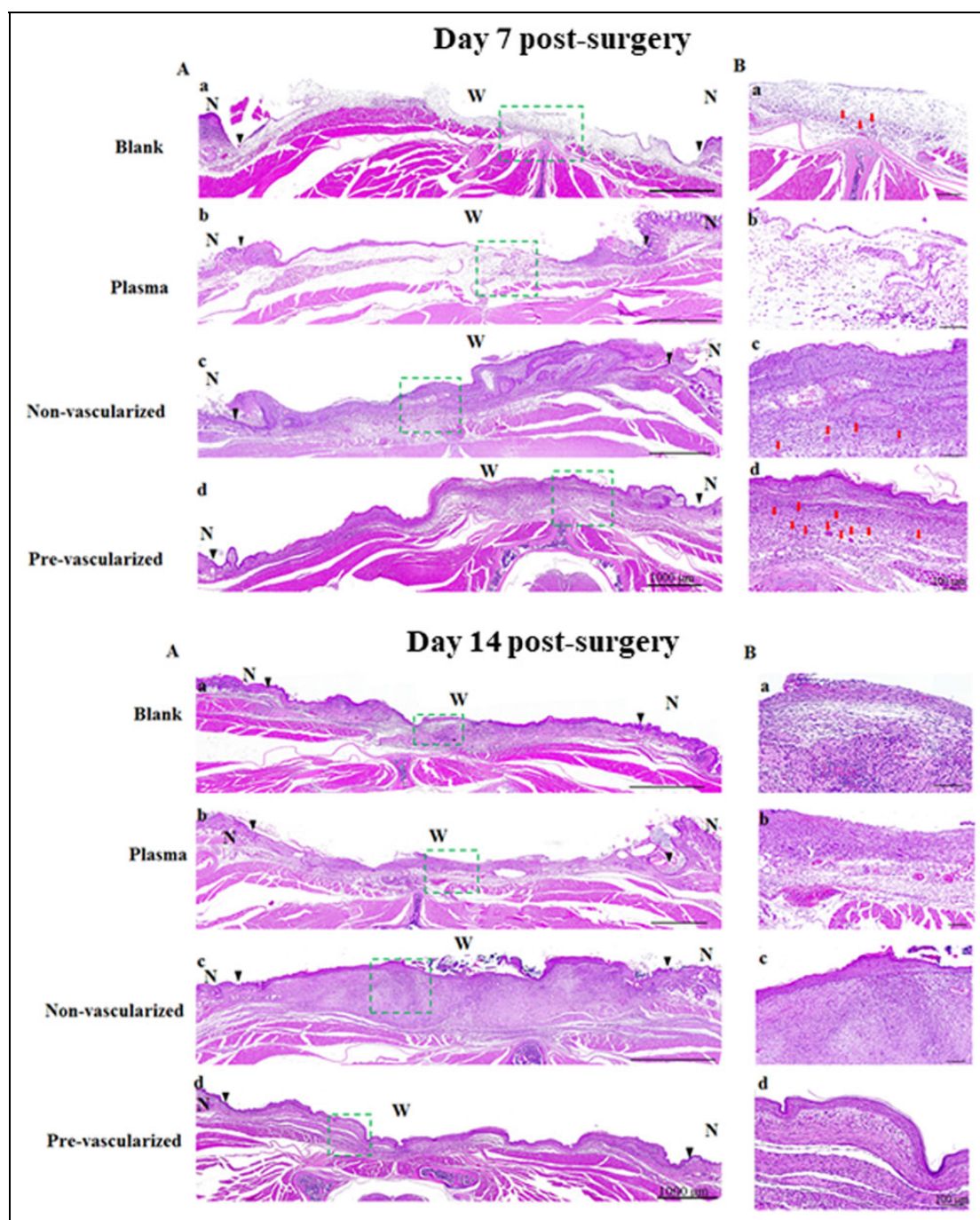


Fig. 6. Histological examination of skin wound healing was observed by H&E staining of the whole skin wound (A) and the center of skin wound (B) wound engrafted by blank (a), plasma gel scaffold (b), non-vascularized (c), and pre-vascularized skin (d) under 20 \times magnification at 7 and 14 days post-surgery. Green dashed rectangle marks the wound center on the dorsal area of nude mice, and the magnification presented as (B) on the right side of images. The epidermal layer could not be found in the blank group. Scale bars = 100 μ m. N indicates normal skin. W indicates wound bed. Black triangles in the images indicate the boundaries between the wound and the surrounding normal skin. Red arrows indicate micro-vessels. $n = 6$ for each group.

Discussion

We successfully prepared a pre-vascularized 3D plasma gel scaffold to promote wound healing and skin regeneration.

UCB plasma gels not only provide a favorable 3D microenvironment for skin dermal fibroblasts and EPCs to grow, but also contribute to epidermal migration, collagen deposition and wound repair. The aim of the present study was to form a

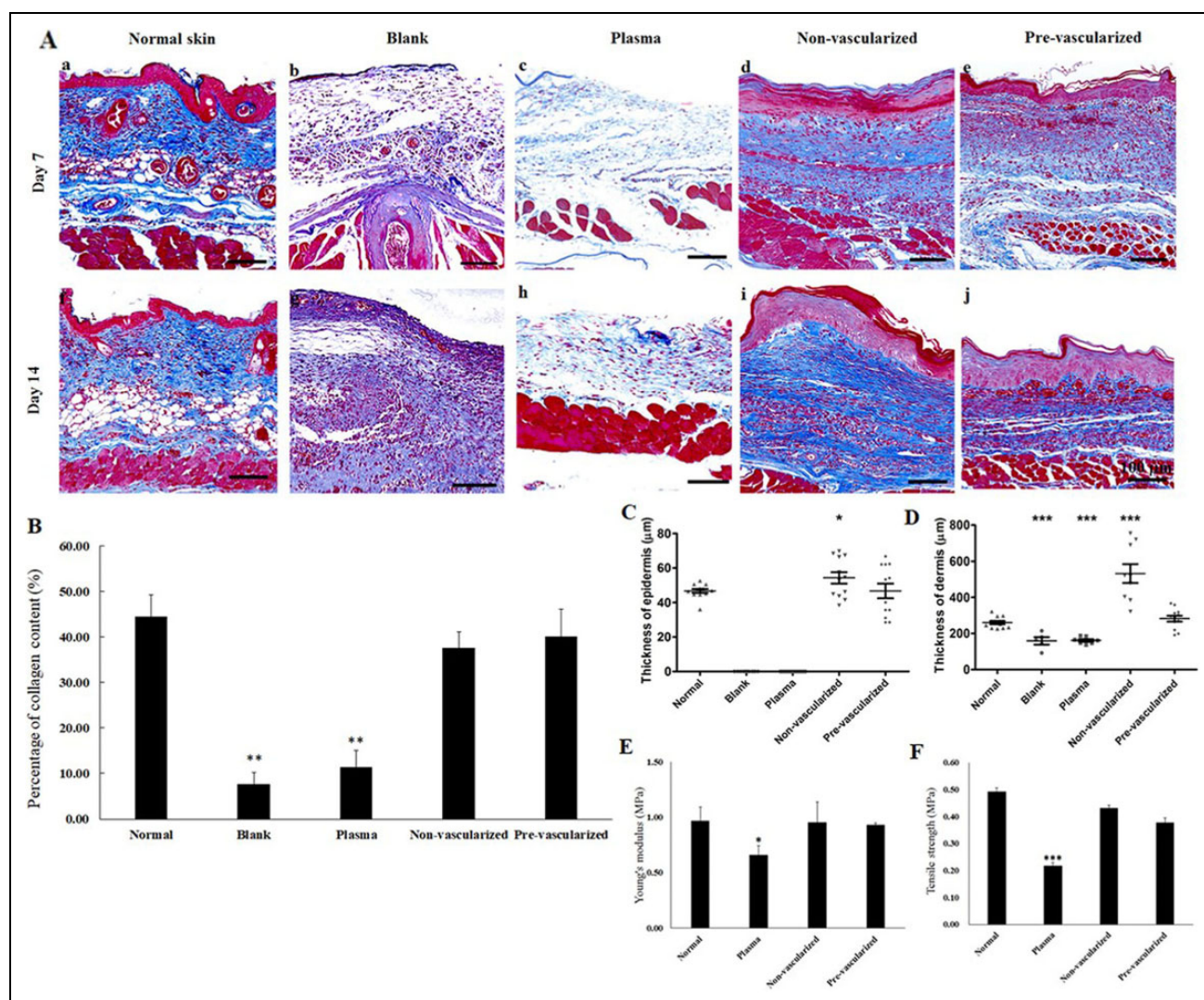


Fig. 7. (A) Masson's trichrome staining for the histological analysis of repaired wound after treatment with blank (b, g), plasma gel scaffold (c, h), non-vascularized skin (d, i), pre-vascularized skin (e, j), and normal skin (a, f) at 7 and 14 days post-surgery. Scale bars = 100 μm. (B) quantification of collagen density after Masson's trichrome staining (C) the calculation of the thickness of the epidermal layer and (D) thickness of the dermal layer as well as the evaluation of mechanical properties measured by (E) Young's modulus and (F) tensile strength 14 days post-surgery in the five groups. *: indicated $P < 0.05$; **: indicates $P < 0.01$; ***: indicates $P < 0.001$ when compared with sham group.

novel skin substitute using EPCs, keratinocytes and fibroblasts within an optimized CaCl_2 cross-linked plasma gel. We modified the CaCl_2 concentrations, EPC-fibroblast co-culture conditions and the ratios of keratinocyte/fibroblasts, and found that the construction of a pre-vascularized 3D skin prior to *in vivo* application is key for successful skin regeneration and wound healing. Although we used plasma and EPC, keratinocytes and fibroblasts derived from different human sources to produce the 3D scaffolds in this study, we aim to apply autologous cells in 3D plasma gels prior to clinical application. In the future, blood from soldiers can be potentially used to produce a plasma gel and to isolate EPCs, to develop a scaffold to treat wounds. This represents a more convenient option when resources are scarce (on the

battlefield), and where blood is available and can be widely used in clinical applications.

In previous studies, high concentrations of CaCl_2 were reported to induce cell apoptosis and inhibit cell growth in the 3D environment¹¹. In the present study, we found that using 10 mM CaCl_2 to construct 3D plasma gel did not compromise cell expansion ability, resulting in a significantly higher cell proliferation rate of fibroblasts over 48 h. In addition, the 10 mM CaCl_2 casted plasma gel provided a suitable niche for the vascularization of EPCs. Establishment of the co-culture system containing both fibroblasts and EPCs was achieved in this study by using mixed cell medium containing 20% FBS, which promoted cell proliferation of both EPCs and fibroblasts. We also found that the

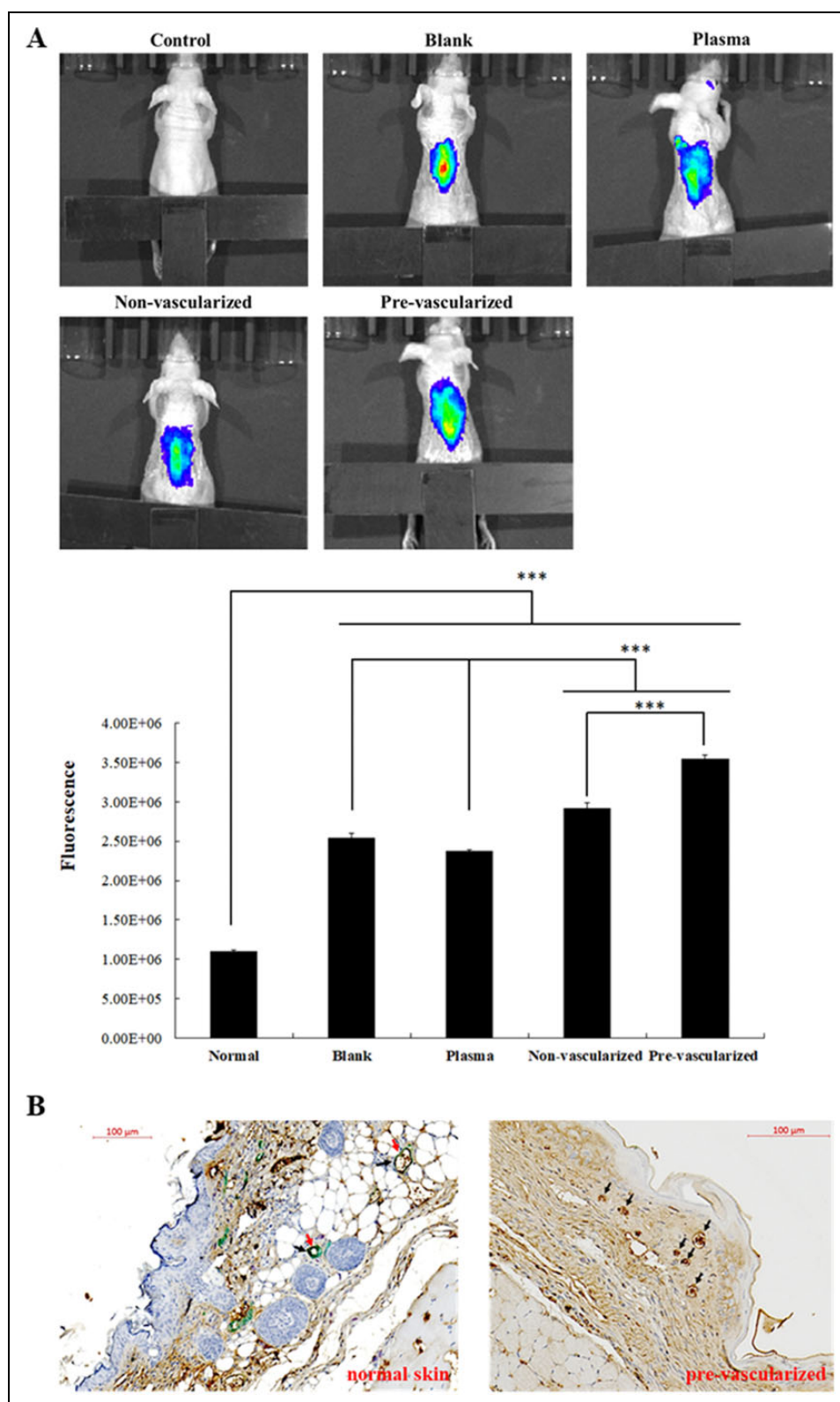


Fig. 8. (A) IVIS imaging of neo-vascular blood perfusion of pre-vascularized 3D gel implants and quantification of fluorescent signals. 14 days after implantation, fluorescence imaging of nude mice were performed using IVIS Spectrum Imaging System as described in the Materials and Methods. *: indicates $P < 0.05$; **: indicates $P < 0.01$; ***: indicates $P < 0.001$. (B) Immunohistochemical staining for normal skin and pre-vascularized skin substitute presenting a vascular-like tubular structure from EPCs on day 14 labeled with CD31 and α SMA markers. CD31 and α SMA were found present in normal skin tissue, while only CD31 labeling was observed in pre-vascularized skin group. CD31: brown, α SMA: green. Black arrows indicate CD31 marker. Red arrows indicate α SMA marker.

micro-vessel network was successfully developed from EPCs, demonstrating a favorable cell culture environment in the 3D plasma gel.

EPCs cultured in 3D systems undergo vascularization, elongation and coalescence for the development of the vascular-like structure containing lumen¹⁶. The formation of the vascular-like structure in 3D culture systems, composed of collagen type I or fibrin, is unique to endothelial cells¹⁷. Previous studies on synthetic hydrogel systems found that the micro-vessel formation of EPCs was influenced by the ratio of endothelial cells to smooth muscle cells¹⁸. From our *in vivo* results of anti- α SMA (HRP green) and anti-CD31 (DAB brown) double staining, we found that EPCs did not differentiate into smooth muscle cells, but formed the neo-vascularization in the wound area after implantation with the pre-vascularized 3D gel scaffold. Based on previous literature, vascular endothelial growth factor is a critical factor for inducing angiogenesis, while basic fibroblast growth factor is a crucial factor for attracting smooth muscle cells¹⁹. In previous studies, smooth muscle alpha-actin was expressed in endothelial cells derived from CD34+ human cord blood cells with medium containing VEGF, bFGF and IGF, implicating these growth factors as critical for smooth muscle cell induction²⁰. We can therefore assume that the production of a microvascular network was not correlated with smooth muscle cell differentiation, perhaps due to the lack of bFGF in human plasma. We evaluated the appropriate ratios of EPCs to fibroblasts in 3D plasma gel scaffolds, and found that a 1:0.5 ratio of EPCs to fibroblasts induced a significantly higher number of micro-vessel formation by day 7. The higher proportion in EPCs showed a higher density of micro-vessel formation in 3D plasma gel, which may be due to the increased cell proliferation rate of fibroblasts that take over space in the 3D gel therefore inhibiting cell differentiation of EPCs. Co-culturing EPCs with fibroblasts is key to the development of vascularization²¹. However, previous reports have suggested that human umbilical vein endothelial cells (HUVEC) alone or the combination of HUVEC and fibroblasts did not support micro-vessel stabilization. Alternatively, it may cause a trophic effect on the host's vascular or epidermal cells in the skin substitutes as the biomaterials could not supply crucial growth factors, such as VEGF and bFGF²². The 3D gel developed in this study provided an adaptive niche for EPCs and fibroblasts that supported cell proliferation, and also enhanced the microvascular network structure and integrity.

Pre-vascularization is a critical factor in tissue engineering and clinical applications^{13,23,24}. Many biomaterial-based scaffolds fail due to poor graft take and integration with host tissue²⁵, or lack neovascularization from the peripheral vessels of the wound edge²⁶. A successful tissue-engineered scaffold is expected to accelerate dermal fibroblast proliferation, collagen deposition, neovascularization and, more importantly, the formation of the epidermal layer. Epidermal coverage of the wound is important as it acts as a barrier

against moisture loss and infection. In this study, the pre-vascularized 3D gel with keratinocytes was engrafted on the wound area of mice. A functional micro-vessel network containing blood flow was apparent in the wound area of mice treated with the pre-vascularized 3D gel scaffold that contributed to accelerated skin regeneration by 14 days post-surgery. Furthermore, the pre-vascularized 3D gel showed mild inflammatory responses. Histological analysis confirmed that the established pre-vascularized network successfully integrated with the surrounding micro-vessels of the wound bed. The epidermal layer was also observed in engrafted pre-vascularized skin by day 7 and 14 post-surgery. On the other hand, dermal thickness was significantly increased in the wounds treated with non-vascularized 3D gel. However, collagen production between non-vascularized and pre-vascularized groups was not significantly different, indicating that the collagen density for pre-vascularized groups was higher than that for non-vascularized groups. Due to the lack of a neo-vascular network in plasma gel, and plasma gel scaffolds seeded with keratinocytes and fibroblasts, we can infer that the original neo-vascular network from the pre-vascularized 3D gel group was gradually integrated into the center of wound 14 days post-surgery. Moreover, our results indicate that the 3D plasma gel scaffold seeded with fibroblasts and keratinocytes can potentially contribute to repairing the wound bed, but the pre-vascularized skin substitute with the EPCs can accelerate the recovery of the skin wound. Based on previous literature, we postulate that the pre-vascularized skin substitute may play a role in shortening the period of vascular regeneration, and may contribute to decreasing hypoxia, inflammation and necrosis during the healing process of the wound bed²⁷. Klar et al. (2017) reported improved outcomes in the early inflammatory response during the early phase of wound healing by the vascularized and non-vascularized bio-engineered dermo-epidermal skin transplants *in vivo*²⁸. Moreover, Ackermann et al. (2014) also demonstrated that priming with proangiogenic growth factors and EPCs enhanced incisional wound healing, by more rapid wound re-epithelialization, higher wound vascularization and higher tensile strength²⁹. Taken together, our data suggest that EPCs play a major role in engrafted pre-vascularized skin substitutes in developing the epidermal and dermal structures to restore normal skin.

Restoring the elasticity of healed skin remains a major challenge in the development of tissue-engineered skin substitutes³⁰. Most manufactured skin substitutes are biocompatible and biodegradable, but do not address requirements for normal skin elasticity. In this study, we confirmed that the mechanical properties of skin engrafted with a plasma gel scaffold were lacking 14 days post-surgery. However, the elasticity of the wounds treated with the non-vascularized and vascularized scaffolds resembled normal skin elasticity.

Conclusions

A novel pre-vascularized plasma gel scaffold was introduced in the present study and was determined a favorable skin substitute to provide multiple requirements, including 3D niche and biocompatibility. Our *in vivo* studies demonstrated that the pre-vascularized 3D gel scaffold can be utilized as a new skin substitute, accelerating epidermal migration and enhancing collagen deposition. Tensile test results also confirmed that engrafted 3D skin substitutes of non-vascularized and pre-vascularized groups were comparable to normal skin elasticity. Therefore, this pre-vascularized 3D skin substitute has great potential in clinical applications for wound repair.

Authors' Note

Dai and Wang contributed equally to this manuscript.

Acknowledgments

Dr. Niann-Tzyy Dai acknowledges the financial support of this work provided by the Ministry of National Defense, ROC (MAB-105-043, MAB-106-034), National Defense Medical Center, Tri-Service General Hospital, ROC (TSGH-C106-112), Zouying Branch of Kaohsiung Armed Forces General Hospital, ROC (ZBH 105-07, ZBH 106-10), Taoyuan Armed Forces General Hospital, ROC (AFTYGH-104-27, AFTYGH-105-27) and Ministry of Science and Technology, ROC (MOST-102-2314-B-016-009, MOST-103-2314-B-016-013). Additional financial support was provided by Teh-Tzer Study Group for Human Medical Research Foundation, ROC. The authors declare no conflicts of interest.

Ethical Approval

The study protocol for the collection of human cells was reviewed and approved by the Institutional Review Board (IRB) in the Tri-Service General Hospital, R.O.C. (TSGHIRB No. 100-05-251).

Statement of Human and Animal Rights

The study protocol for the collection of human cells was reviewed and approved by the Institutional Review Board (IRB) in the Tri-Service General Hospital, R.O.C. (TSGHIRB No. 100-05-251). A written informed consent according to the guidelines of Institutional Review Board (IRB) was obtained from each donor. In addition, the protocol for animal experiment was approved by the Institutional Animal Care and Use Committee (IACUC) in National Defense Medical Center, Taiwan, R.O.C. (IACUC-14-286).

Statement of Informed Consent

The study protocol for the collection of human cells was reviewed and approved by the Institutional Review Board (IRB) in the Tri-Service General Hospital, R.O.C. (TSGHIRB No. 100-05-251). A written informed consent according to the guidelines of Institutional Review Board (IRB) was obtained from each donor.


Declaration of Conflicting Interests

The authors declared no potential conflicts of interest with respect to the research, authorship, and/or publication of this article.

Funding

The authors disclosed receipt of the following financial support for the research, authorship, and/or publication of this article: Ministry of National Defense, ROC (MAB-105-043, MAB-106-034), National Defense Medical Center, Tri-Service General Hospital, ROC (TSGH-C106-112), Zouying Branch of Kaohsiung Armed Forces General Hospital, ROC (ZBH 105-07, ZBH 106-10), Taoyuan Armed Forces General Hospital, ROC (AFTYGH-104-27, AFTYGH-105-27) and Ministry of Science and Technology, ROC (MOST-102-2314-B-016-009, MOST-103-2314-B-016-013). Additional financial support was provided by Teh-Tzer Study Group for Human Medical Research Foundation, ROC.

ORCID iD

Niann-Tzyy Dai  <http://orcid.org/0000-0003-2066-574X>

Supplemental Material

Supplemental material for this article is available online.

References

1. Pellegrini G, Ranno R, Stracuzzi G, Bondanza S, Guerra L, Zambruno G, Micali G, De Luca M. The control of epidermal stem cells (holoclones) in the treatment of massive full-thickness burns with autologous keratinocytes cultured on fibrin. *Transplantation*. 1999;68(6):868–879.
2. Takeo M, Lee W, Ito M. Wound healing and skin regeneration. *Cold Spring Harb Perspect Med*. 2015;5(1):a023267.
3. Bottcher-Haberzeth S, Biedermann T, Reichmann E. Tissue engineering of skin. *Burns*. 2010;36(4):450–460.
4. Murphy SV, Skardal A, Atala A. Evaluation of hydrogels for bio-printing applications. *J Biomed Mater Res A*. 2013;101(1):272–284.
5. Lee V, Singh G, Trasatti JP, Bjornsson C, Xu X, Tran TN, Yoo SS, Dai G, Karande P. Design and fabrication of human skin by three-dimensional bioprinting. *Tissue Eng Part C Methods*. 2014;20(6):473–484.
6. Bard JB, Hay ED. The behavior of fibroblasts from the developing avian cornea. Morphology and movement in situ and in vitro. *J Cell Biol*. 1975;67(2PT.1):400–418.
7. Ju YE, Janmey PA, McCormick ME, Sawyer ES, Flanagan LA. Enhanced neurite growth from mammalian neurons in three-dimensional salmon fibrin gels. *Biomaterials*. 2007;28(12):2097–2108.
8. Wong T, McGrath JA, Navsaria H. The role of fibroblasts in tissue engineering and regeneration. *Br J Dermatol*. 2007;156(6):1149–1155.
9. Moon JJ, West JL. Vascularization of engineered tissues: approaches to promote angio-genesis in biomaterials. *Curr Top Med Chem*. 2008;8(4):300–310.
10. Asahara T. [Endothelial progenitor cells for vascular medicine]. *Yakugaku Zasshi*. 2007;127(5):841–845.
11. Abe Y, Ozaki Y, Kasuya J, Yamamoto K, Ando J, Sudo R, Ikeda M, Tanishita K. Endothelial progenitor cells promote directional three-dimensional endothelial network formation by secreting vascular endothelial growth factor. *PLoS One*. 2013;8(12):e82085.

12. Peters EB, Liu B, Christoforou N, West JL, Truskey GA. Umbilical cord blood-derived mononuclear cells exhibit pericyte-like phenotype and support network formation of endothelial progenitor cells in vitro. *Ann Biomed Eng.* 2015; 43(10):2552–2568.
13. Huang SP, Hsu CC, Chang SC, et al. Adipose-derived stem cells seeded on acellular dermal matrix grafts enhance wound healing in a murine model of a full-thickness defect. *Ann Plast Surg.* 2012;69(6):656–662.
14. Akturk O, Tezcaner A, Bilgili H, Deveci MS, Gecit MR, Keskin D. Evaluation of sericin/collagen membranes as prospective wound dressing biomaterial. *J Biosci Bioeng.* 2011; 112(3):279–288.
15. Desai S, Srambikkal N, Yadav HD, Shetake N, Balla MM, Kumar A, Ray P, Ghosh A, Pandey BN. Molecular understanding of growth inhibitory effect from irradiated to bystander tumor cells in mouse fibrosarcoma tumor model. *PLoS One.* 2016;11(8):e0161662.
16. Madri JA, Pratt BM. Endothelial cell-matrix interactions: in vitro models of angiogenesis. *J Histochem Cytochem.* 1986; 34(1):85–91.
17. Hirschi KK, Ingram DA, Yoder MC. Assessing identity, phenotype, and fate of endothelial progenitor cells. *Arterioscler Thromb Vasc Biol.* 2008;28(9):1584–1595.
18. Peters EB, Christoforou N, Leong KW, Truskey GA, West JL. Poly(ethylene glycol) hydrogel scaffolds containing cell-adhesive and protease-sensitive peptides support microvessel formation by endothelial progenitor cells. *Cell Mol Bioeng.* 2016;9(1):38–54.
19. Huang C, Orbay H, Tobita M, Miyamoto M, Tabata Y, Hyakusoku H, Mizuno H. Proapoptotic effect of control-released basic fibroblast growth factor on skin wound healing in a diabetic mouse model. *Wound Repair Regen.* 2016;24(1):65–74.
20. Lu X, Dunn J, Dickinson AM, Gillespie JJ, Baudouin SV. Smooth muscle alpha-actin expression in endothelial cells derived from CD34+ human cord blood cells. *Stem Cells Dev.* 2004;13(5):521–527.
21. Vitacolonna M, Belharazem D, Hohenberger P, Roessner ED. In-vivo quantification of the revascularization of a human acellular dermis seeded with EPCs and MSCs in co-culture with fibroblasts and pericytes in the dorsal chamber model in pre-irradiated tissue. *Cell Tissue Bank.* 2017;18(1):27–43.
22. Hendrickx B, Vranckx JJ, Luttun A. Cell-based vascularization strategies for skin tissue engineering. *Tissue Eng Part B Rev.* 2011;17(1):13–24.
23. Chen X, Aledia AS, Ghajar CM, Griffith CK, Putnam AJ, Hughes CC, George SC. Prevascularization of a fibrin-based tissue construct accelerates the formation of functional anastomosis with host vasculature. *Tissue Eng Part A.* 2009;15(6): 1363–1371.
24. Du P, Suhaeri M, Ha SS, Oh SJ, Kim SH, Park K. Human lung fibroblast-derived matrix facilitates vascular morphogenesis in 3D environment and enhances skin wound healing. *Acta Biomater.* 2017;54:333–344.
25. Zhang W, Wray LS, Rnjak-Kovacina J, Xu L, Zou D, Wang S, Zhang M, Dong J, Li G, Kaplan DL, Jiang X. Vascularization of hollow channel-modified porous silk scaffolds with endothelial cells for tissue regeneration. *Biomaterials.* 2015; 56:68–77.
26. Xiong S, Zhang X, Lu P, Wu Y, Wang Q, Sun H, Heng BC, Bunpetch V, Zhang S, Ouyang H. A gelatin-sulfonated silk composite scaffold based on 3D printing technology enhances skin regeneration by stimulating epidermal growth and dermal neovascularization. *Sci Rep.* 2017;7(1):4288.
27. Frueh FS, Menger MD, Lindenblatt N, Giovanoli P, Laschke MW. Current and emerging vascularization strategies in skin tissue engineering. *Crit Rev Biotechnol.* 2017; 37(5):613–625.
28. Klar AS, Biedermann T, Simmen-Meuli C, Reichmann E, Meuli M. Comparison of in vivo immune responses following transplantation of vascularized and non-vascularized human dermo-epidermal skin substitutes. *Pediatr Surg Int.* 2017; 33(3):377–382.
29. Ackermann M, Pabst AM, Houdek JP, Ziebart T, Konerding MA. Priming with proangiogenic growth factors and endothelial progenitor cells improves revascularization in linear diabetic wounds. *Int J Mol Med.* 2014;33(4):833–839.
30. Yang TL. Chitin-based materials in tissue engineering: applications in soft tissue and epithelial organ. *Int J Mol Sci.* 2011; 12(3):1936–1963.